Acta Crystallographica Section D
Biological Crystallography
ISSN 0907-4449

Crystallization and phasing of focal adhesion protein 52 from *Gallus gallus*

Imre Törő,[a] Marko Nikki,[b] Tuomo Glumoff,[c] Veli-Pekka Lehto[d] and Kristina Djinović Carugo[a]*

[a]Structural Biology Laboratory, ELETTRA – Sincrotrone Trieste in Area Science Park, S.S. 14 Km 163, 5 loc. Basovizza, 34012 Trieste, Italy, [b]Department of Pathology, University of Oulu, FIN-90014, Finland, [c]Department of Biochemistry, University of Oulu, FIN-90014, Finland, and [d]Department of Pathology, University of Helsinki and Helsinki University Central Hospital, Helsinki FIN-00290, Finland

Correspondence e-mail: djinovic@elettra.trieste.it

Received 12 November 2003
Accepted 17 December 2003

Focal adhesion protein 52 (FAP52) is a multidomain adaptor protein of 448 amino acids characterized as an abundant component of focal adhesions. FAP52 binds to filamin *via* its N-terminal α-helical domain, suggesting a role in linking focal adhesions to the actin-based cytoskeleton. The recombinant protein was crystallized using the hanging-drop vapour-diffusion method, which yielded two crystal forms. Native data were collected from both crystal forms to 2.8 and 2.1 Å resolution, respectively. For one of the crystal forms, initial MAD phasing was successfully performed using two data sets from xenon-derivatized crystals. The derivative data sets were collected using softer X-rays of 1.5 and 1.9 Å wavelength. Preliminary structural analysis reveals the presence of a dimer in the asymmetric unit.

1. Introduction

FAP52 is a focal adhesion-associated protein of molecular weight 52 kDa (Meriläinen *et al.*, 1997). It co-localizes with several cytoskeletal proteins such as vinculin, talin and paxillin. FAP52 consists of three distinct domains: an N-terminal α-helical domain is connected to a C-terminal SH3 domain through an unstructured linker region. FAP52 shares high sequence homology with about a dozen proteins, which form the PCH (pombe Cdc15 homology) protein family (Lippincott & Li, 2000). PCH-family members are also characterized by the presence of a FER-CIP4 homology (FCH) domain at their very N-terminus. The central α-helical part of the molecule was predicted to adopt a coiled-coil structure and to consequently form oligomers. Indeed, *in vitro* experiments have shown that FAP52 presumably oligomerizes by forming trimers (Nikki *et al.*, 2002*a*). The oligomerization interface was identified by stepwise truncation of the protein from both the N- and C-termini and by analyzing the self-association of these constructs. The amino-acid residues required for self-association of FAP52 subunits coincide well with the central region predicted to form coiled coil. Recently, filamin of molecular weight 280 kDa (ABP-280) was identified as a binding partner of FAP52 as it co-immunoprecipitates with FAP52 upon the addition of anti-FAP52 antibodies to cell extracts (Nikki *et al.*, 2002*b*). The regions in the two proteins that contribute to complex formation were elucidated by monitoring the binding affinity of various N- and C-terminally truncated constructs of FAP52 and filamin. These experiments showed that the α-helical N-terminal domain of FAP52 and repeat 15 of filamin are necessary for complex formation (Nikki *et al.*, 2002*b*).

2. Materials and methods

2.1. Cloning and expression

The identification and cloning of FAP52 from a chicken cDNA library is described in Meriläinen *et al.* (1997). The full-length cDNA encoding FAP52 was inserted into a pGEX-2TK vector (Amersham Biosciences), which was then used to transform *Escherichia coli* BL21(DE3) cells. The recombinant protein was expressed in bacteria by standard procedures. The cells were then pelleted by centrifugation and resuspended in cold PBS buffer containing aprotinin at a concentration of 3 µmol l^{-1}. The cells were gently lysed by sonication and the supernatant was separated from the cell debris by centrifugation. Glutathione-Sepharose 4B beads were added to the supernatant in order to remove the GST-FAP52 fusion protein from the solution. After equilibration, the beads were packed into an empty column, washed with five column volumes of cold PBS additionally containing 0.5 *M* NaCl and then washed again with two column volumes of cold PBS buffer. Cleaving FAP52 from the GST-fusion protein was achieved on the column by the addition of bovine thrombin (10 units of thrombin per milligram of fusion protein; Amersham Biosciences) and incubation for 10 min. The reaction was stopped by adding PMSF, benzamidine and leupeptin to achieve final concentrations of 0.25, 5 and 1 m*M*, respectively. FAP52 was eluted from the column with cold

PBS buffer. The eluted protein was purified to homogeneity on a MonoQ column (Amersham Biosciences) by using an NaCl gradient and bis-Tris buffer adjusted to pH 6.0. The purified protein was dialyzed against 20 m*M* Tris–HCl pH 8 by three cycles of dilution-concentration from 15 to 1 ml using an Amicon Centriprep concentration column (Millipore). The final concentration of the solution was adjusted to 13.5 mg ml^{-1}.

2.2. Crystallization

The hanging-drop vapour-diffusion technique was used for all crystallization experiments. Drops were prepared by mixing 1 µl protein solution (prepared as above) with 1 µl well solution and were suspended over 1 ml reservoir solution. Ammonium Sulfate Grid Screen (Hampton Research) was tested in initial trials at 293 K with immediate success: small crystals appeared after 1 d of equilibration. However, further optimization did not yield sufficiently large crystals. In subsequent screens, combinations of polyethylene glycol (PEG) and ammonium sulfate (AS) were employed as precipitating agents. PEG 2000 MME was used in the concentration range 10–30%, while the AS concentration was varied from 100 to 400 m*M* in 50 m*M* steps. The drops were buffered with 100 m*M* HEPES pH 8.0, which seemed to be the best pH value as deduced from the initial screens with AS. Single crystals suitable for diffraction experiments were grown under the following conditions: 20–22% PEG 2000 MME, 350 m*M* AS and 100 m*M* HEPES pH 8.0. Two crystal forms clearly distinguishable by their different morphologies (Fig. 1) grew simultaneously in the same drops. Form I has the shape of columns or thick needles, while form II appears as prism/plate-shaped crystals.

2.3. Data collection and processing

A uniform cryoprotectant solution with the following components was used for all the experiments: 25% PEG 2000 MME, 200 m*M* AS, 100 m*M* HEPES pH 8.0 and 15% glycerol. Crystals were briefly soaked in the cryoprotectant solution, flash-cooled in liquid nitrogen and transported in a Dewar under liquid nitrogen to the synchrotron beamlines. All data collections were performed at 100 K using a 700 Series Oxford Cryosystems cooling device (Oxford Cryosystems, 2000).

2.3.1. Crystal form I. Form 1 crystals belong to space group $P2_12_12_1$. 120° of rotation data from a native crystal were collected using a 1° oscillation angle on beamline ID14-1 at ESRF using an ADSC Quantum 4 CCD detector. The best crystal diffracted to a resolution of 2.8 Å (Table 1).

2.3.2. Crystal form II. Form 2 crystals belong to space group *C*2. In this case, 180° of rotation data from a native crystal were collected using a 1° oscillation angle on beamline ID14-2 at ESRF using an ADSC Quantum 4 CCD detector. The best crystal diffracted to a resolution of 2.1 Å (Table 1). In addition, a 3.27 Å low-resolution data set consisting of 54 frames with a 3° oscillation angle were collected to supplement the missing low-resolution reflections lost owing to overload.

Table 1
Data-collection and MIRAS statistics for native crystal forms I and II and the xenon-derivatized crystal form I of FAP52.

Values in parentheses are for the highest resolution shell.

			Xenon-derivatized crystals (form I)	
	Native (form I)	Native (form II)	Collected at 1.5 Å	Collected at 1.9 Å
Crystal data				
Space group	$P2_12_12_1$	*C*2	$P2_12_12_1$	$P2_12_12_1$
Unit-cell parameters				
a (Å)	101.4	164.7	101.8	101.1
b (Å)	105.9	102.2	106.00	104.8
c (Å)	126.3	107.3	126.0	124.9
β (°)	—	131.2	—	—
Reflecting range† (°)	1.38	2.01	2.74	2.15
Data collection and phasing				
Beamline	ID14-1 (ESRF)	ID14-2 (ESRF)	XRD1 (ELETTRA)	XRD1 (ELETTRA)
Wavelength (Å)	0.934	0.933	1.500	1.900
Resolution range (Å)	30–2.8 (2.98–2.8)	30–2.1 (2.22–2.1)	30–2.99 (3.17–2.99)	30–3.0 (3.18–3.0)
Observed reflections	161537	243066	108475	98084
Unique reflections	33241	70602	47707	44969
$R_{\rm merge}$‡	0.071 (0.334)	0.071 (0.295)	0.054 (0.149)	0.068 (0.308)
Completeness (%)	97.3 (90.7)	90.0 (59.3)	89.6 (57.0)	87.6 (84.8)
$\langle I/\sigma(I)\rangle$	14.6 (4.8)	10.1 (2.6)	12.4 (4.9)	10.6 (3.2)
Phasing power§				
Isomorphous (centric/acentric)	—	—	—	0.451/0.510
Anomalous	—	—	0.842	0.830
$R_{\rm Cullis}$¶ (iso/ano)	—	—	—/0.861	0.349/0.886

† Reflecting range as defined in the *XDS* manual: 'angular lifetime (°) of a reflection to pass completely through the Ewald sphere on the shortest route'. ‡ $R_{\rm merge} = \sum|I_i - \langle I_i\rangle|/\sum\langle I_i\rangle$, where I_i is the observed intensity and $\langle I_i\rangle$ is the average intensity over symmetry-equivalent intensities. § Isomorphous phasing power, $[\sum|F_H({\rm calc})|^2/\sum|E|^2]^{1/2}$, where $\sum|E|^2 = \sum[|F_{PH}({\rm obs})| - |F_{PH}({\rm calc})|]^2$; anomalous phasing power, $[\sum|F_H({\rm imag})|^2/\big||\Delta F^{\pm}_{PH}({\rm obs})| - |\Delta F^{\pm}_{PH}({\rm calc})|\big|^2]^{1/2}$, where $\Delta F^{\pm}_{PH}$ is the structure-factor difference between Bijvoet pairs and F_H(imag) is the imaginary component of the calculated structure-factor contribution by the anomalously scattering atoms. ¶ $R_{\rm Cullis}({\rm iso}) = \sum\big||F_{PH} \pm F_P| - F_H({\rm calc})\big|/\sum|F_{PH} \pm F_P|$; $R_{\rm Cullis}({\rm ano}) = \sum\big||\Delta F^{\pm}_{PH}({\rm obs})| - |\Delta F^{\pm}_{PH}({\rm calc})|\big|/\Delta F^{\pm}_{PH}({\rm obs})$.

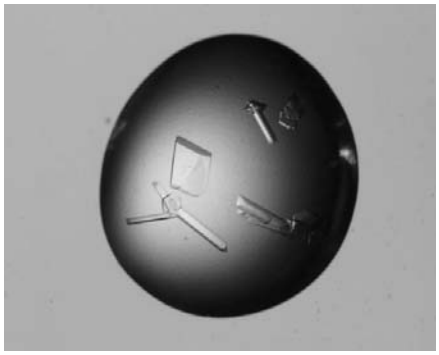

Figure 1
Two different crystal forms of FAP52 in one drop (the diameter of the drop is approximately 2–2.5 mm).

2.3.3. Xenon derivatives. The xenon derivative was generated by subjecting crystals of form I to 1.4–1.5 MPa xenon for 5–7 min in a commercially available chamber from Oxford Cryosystems (Xcell). The crystals were briefly soaked in a cryoprotectant solution prior to mounting them in cryoloops (Hampton Research) and inserting them into the pressure cell. After releasing the pressure, the crystals were rapidly plunged into liquid nitrogen to avoid desorption of xenon. Data from xenon-derivatized crystals were collected on the tuneable XRD1 beamline at ELETTRA using 1.5 and 1.9 Å wavelengths. In both cases 110° of data were acquired to a maximum resolution of 3 Å. 15° of data had to be discarded from the data set collected with 1.9 Å wavelength owing to equipment error.

All data were processed with *XDS* and scaled with *XSCALE* (Kabsch, 1993). The native data were converted to *CNS* format using *XDSCONV*, which in turn was converted to the *CCP*4 MTZ format using *F2MTZ* (Collaborative Computational Project, Number 4, 1994). The anomalous xenon-derivative data were converted to MTZ format by a Perl script xds2mtz.pl written by Serge Cohen (available for download at http://www.yorvic.york.ac.uk/ccp4bb/2002/msg00165.html), which also

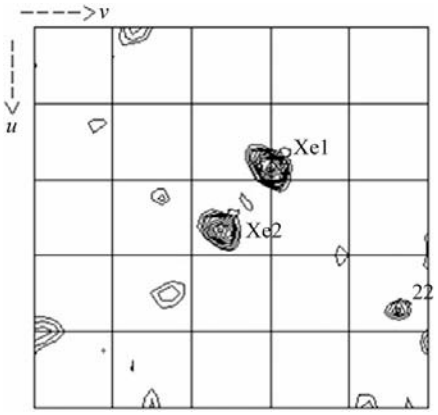

Figure 2
The Harker section at w = 1/2 of an anomalous Patterson map calculated with diffraction data in the range 30–4 Å resolution, contoured in steps of 0.5σ starting at 1.5σ. The map limits are u = 0–1/2 and v = 0–1/2 . The xenon Harker peaks are indicated (Xe1, Xe2).

employs *XDSCONV* and *F2MTZ*. Data-collection and processing statistics are reported in Table 1.

2.4. Phasing

The positions of two Xe atoms were determined using *RSPS* (Collaborative Computational Project, Number 4, 1994) from an anomalous Patterson map calculated from the data set collected using 1.9 Å wavelength (Fig. 2). The resulting coordinates were input into *SHARP* (de La Fortelle & Bricogne, 1997) in order to calculate experimental phases and to locate additional Xe atoms in an iterative way. The final experimental map from *SHARP* was solvent-flattened with *SOLOMON* (Abrahams & Leslie, 1996; Collaborative Computational Project, Number 4, 1994).

3. Results and discussion

FAP52 shows polymorphism, with two crystal forms growing simultaneously in the same hanging drop. Crystal form I belongs to space group $P2_12_12_1$. The column-shaped crystals nucleate in a couple of days, reaching final average dimensions of 500 × 60 × 60 µm. The volume of the unit cell is 1.36×10^6 Å^3, which permits two or three protein molecules per asymmetric unit (V_M = 3.3 Å^3 Da^{-1} in the case of two molecules and 2.2 Å^3 Da^{-1} in the case of three). Form I is the predominant crystal form in PEG conditions and is also the more resistant to mechanical shock, making pressurization with xenon gas possible without loss of diffraction, although the crystal mosaicity increases significantly (see Table 1).

Form II crystals belong to space group $C2$. The prisms or rhomboidal plates grow less commonly than the form I crystals and have average dimensions of 250 × 250 × 100 µm. The volume of the unit cell is 1.36×10^6 Å^3, which like form I is consistent with the presence of two or three molecules per asymmetric unit. These crystals are particularly fragile, breaking easily during the mounting manipulations. Trials to obtain xenon-derivatized crystals of form II failed completely as the diffraction pattern was seriously compromised in each case. The native data set collected from form II crystals at ESRF showed signs of radiation damage. Therefore, 30 frames at the end of the data set were omitted from the processing.

The data sets from xenon-derivatized crystals were collected to a maximum resolution of 3 Å from two different crystals using wavelengths of 1.5 and 1.9 Å. The isomorphous Patterson maps calculated from the differences of the native and xenon-derivatized data sets of form I crystals were uninterpretable owing to lack of isomorphism. Therefore, anomalous Patterson maps were generated in order to locate the initial set of two heavy-atom positions. A MAD phasing scenario was then set up in *SHARP* (de La Fortelle & Bricogne, 1997) with an initially incomplete heavy-atom model: the 1.5 Å xenon data set was used as a reference against the 1.9 Å xenon data set. The fact that the two xenon data sets were collected from two different crystals was properly implemented in the *SHARP* setup. The starting occupancies for the Xe atoms were set to the more realistic value of 0.5. After a complete refinement cycle, inspection of the anomalous residual maps revealed three additional xenon sites. Interestingly, four of the five Xe atoms are bound to the protein as two pairs with distances of 3.3 and 3.7 Å between the atoms forming the pairs. The second refinement cycle with the updated heavy-atom substructure did not reveal any new sites; the atoms located by *RSPS* had to be refined with anisotropic B factors in a final refinement. At present, the overall figure of merit (FOM) is 0.32 and 0.12 for acentric and centric reflections, respectively. The experimental electron-density map was not readily interpretable and was therefore solvent-flattened by *SOLOMON* using an option in the web interface of *SHARP* (*SUSHI*) to search for an optimal solvent envelope. This optimization was carried out by running *SOLOMON* with various solvent-content values while calculating various quality indicators. The inspection of the solvent-flattened electron-density maps and the position of the xenon sites suggested the presence of twofold non-crystallographic symmetry. The NCS operator was found by a procedure implemented in *SUSHI* using a combination of the programs *POLARRFN* (Collaborative Computational Project, Number 4, 1994), *GETAX* (Vonrhein & Schulz, 1999; Collaborative Computational Project, Number 4, 1994) and *DM* (Cowtan, 1994; Collaborative Computational Project, Number 4, 1994). Although the self-rotation function did not reveal any peaks except that of the origin, *GETAX* found the NCS rotation axis almost parallel to one of the crystallographic axes, which was confirmed by twofold averaging in *DM*. The inspection of the solvent-flattened and averaged electron-density maps suggests that the phases will be sufficient to ultimately allow structure determination of FAP52.

We wish to thank Joanne McCarthy and Stéphanie Monaco at ESRF for their assistance at the ID14-1 and ID14-2 beamlines. Many thanks to Gwyndaf Evans at Global Phasing Ltd for help in the initial phasing with *SHARP*. Maurizio Polentarutti (ELETTRA) is kindly acknowledged for help with the pressure cell and xenon-derivatization of crystals. IT is a recipient of a Longterm Postdoctoral Fellowship from the European Molecular Biology Organization, Heidelberg, Germany. In the early stages of this work IT was supported by a TRIL fellowship from the International Centre of Theoretical Physics, Trieste, Italy.

References

Abrahams, J. P. & Leslie, A. G. W. (1996). *Acta Cryst.* D**52**, 30–42.
Collaborative Computational Project, Number 4 (1994). *Acta Cryst.* D**50**, 760–763.
Cowtan, K. (1994). *Jnt CCP4/ESF–EACBM Newsl. Protein Crystallogr.* **31**, 34–38.
Kabsch, W. (1993). *J. Appl. Cryst.* **26**, 795–800.
La Fortelle, E. de & Bricogne, G. (1997). *Methods Enzymol.* **276**, 472–494.
Lippincott, J. & Li, R. (2000). *Microsc. Res. Tech.* **49**, 168–172.
Meriläinen, J., Lehto, V.-P. & Wasenius, V.-M. (1997). *J. Biol. Chem.* **272**, 23278–23284.
Nikki, M., Meriläinen, J. & Lehto, V.-P. (2002*a*). *Biochemistry*, **41**, 6320–6329.
Nikki, M., Meriläinen, J. & Lehto, V.-P. (2002*b*). *J. Biol. Chem.* **277**, 11432–11440.
Oxford Cryosystems (2000). *Acta Cryst.* D**56**, 380.
Vonrhein, C. & Schulz, G. E. (1999). *Acta Cryst.* D**55**, 225–229.